



Immunogenic potential and neutralizing ability of a heterologous version of the most abundant three-finger toxin from the coral snake *Micrurus mipartitus*

Luz Elena Romero Giraldo^{1*} , Sergio Pulido^{2,3}, Mario Andrés Berrío^{2,3}, María Fernanda Flórez², Paola Rey-Suárez^{1,4} , Vitelbina Núñez-Rangel^{1,5}, Mónica Saldarriaga Córdoba⁴, Jaime Andrés Pereañez¹

¹Research Group in Toxinology, Pharmaceutical, and Food Alternatives, University of Antioquia, Medellín, Colombia.

²LifeFactors Free Zone SAS, Rionegro, Antioquia, Colombia.

³Tropical Disease Study and Control Program – PECET, University of Antioquia, Medellín, Colombia.

⁴Center for Research in Natural Resources and Sustainability, Bernardo O'Higgins University, Santiago, Chile.

⁵Microbiology School, University of Antioquia, Medellín, Colombia.

Keywords:

Recombinant protein
Antibodies
Micrurus mipartitus
Coral snake antivenoms
Three-finger toxin
Mipartoxin-1

Abstract

Background: *Micrurus mipartitus* is a coral snake of public health concern in Colombia. Its venom is mainly composed of three-finger toxins (3FTxs), Mipartoxin-1 being the most abundant protein partially responsible for its lethal effect. In this work, we present the production of Mipartoxin-1 in a recombinant form and evaluate its immunogenic potential. **Methods:** A genetic construct HisrMipartoxin-1 was cloned into the pET28a vector and heterologous expression was obtained in *E. coli* BL21 (DE3). The recombinant HisrMipartoxin-1 protein was extracted from inclusion bodies, refolded *in vitro*, and isolated by affinity and RP-HPLC chromatography. The lethal effect of HisrMipartoxin-1 was tested, and antibodies against HisrMipartoxin-1 were produced by immunization in rabbits. The antibody titers were monitored by an ELISA test. The neutralizing ability of the antibodies, against the lethal effect of native toxins and *M. mipartitus* venom, was also assessed. **Results:** HisrMipartoxin-1 was detected on SDS-PAGE, with a molecular mass of around 11 kDa. The retention time was 16.0 minutes. HisrMipartoxin-1 did not exhibit lethality in mice; however, antibodies against HisrMipartoxin-1 recognized the native toxin, the whole venom of *M. mipartitus*, and a 3FTx from another species within the *Micrurus* genus. Furthermore, antibodies against HisrMipartoxin-1 completely neutralized the lethal effect of native Mipartoxin-1 in mice but not *M. mipartitus* whole venom. **Conclusion:** These findings indicate that HisrMipartoxin-1 might be used as an immunogen to develop anticoral antivenoms or complement them. This work is the first report of the heterologous expression of 3FTx from *M. mipartitus*.

* Correspondence: luze.romero@udea.edu.co

<https://doi.org/10.1590/1678-9199-JVATITD-2023-0074>

Received: 26 September 2023; Accepted: 13 March 2024; Published online: 25 November 2024



Background

According to the World Health Organization (WHO), snakebite envenoming is a neglected disease and a severe public health problem that affects tropical and subtropical regions globally [1]. Millions of snakebite envenoming cases have been estimated worldwide, about 1.8–2.7 million people per year [2], with an estimated 81,000 to 138,000 deaths annually [1]. Of these, 137,000–150,000 envenomings and 3,400–5,000 deaths occur in Latin America and the Caribbean [2]. The Instituto Nacional de Salud (INS) of Colombia reported 5573 cases of snakebites in the year 2022, 1.3% being inflicted by coral snakes [3].

Coral snakes of the genus *Micrurus* (Wagler, 1824) are the representatives of the Elapidae family across the Americas, from the southern United States to Argentina [4]. Coral snakes have proteroglyphous fangs that allow them to inject venom and induce an envenomation that is characterized by neurotoxic effects such as bilateral ptosis and progressive respiratory paralysis [5]. According to Lomonte et al. [6] *Micrurus* venoms are predominantly composed of three-finger toxins (3FTxs) and Phospholipases A₂ (PLA₂s), the 3FTxs being the predominant proteins in *M. mipartitus* venom (~60% of total proteins) [7]. This species is widely distributed in Colombia and is commonly named ‘redtail coral snake’ or ‘rabo de aji’ [7]. Rey-Suárez et al. [8] identified Mipartoxin-1 (UniProt: B3EWF8) as the most abundant 3FTx from *M. mipartitus* venom (28%) and presents four isoforms [9]. Mipartoxin-1 is a short-chain (or “type-I”) α -neurotoxin of molecular mass 7030 Da and has a highly lethal activity in mice (LD50: 0.06 μ g/g) [8]. Moreover, Mipartoxin-1 plays an important role in venom toxicity, contributing significantly to neurotoxic manifestations by causing neuromuscular blockade of post-synaptic nicotinic receptors, as was evidenced in both avian and mammalian preparations [8].

The standard treatment of coral snakebite is the administration of antivenom [10–14]. In Colombia, the National Institute of Health (INS) produces the Polyvalent Anticoral Antivenom, which is composed of equine immunoglobulins that neutralize the venom of *M. dumerilii*, *M. mipartitus*, *M. isozonus*, *M. surinamensis* and *M. lemniscatus*, *M. spixii* and *M. medemi* [15]. However, it is known that *M. mipartitus* and *M. dumerilii*, whose compositional dichotomy of their venoms differs between 3FTxs and PLA₂, respectively, are the cause of most envenomings by coral snakes in Colombia [5, 7]. For this reason, it has been shown that, in some cases, the lethality of the venom has not been neutralized [16, 17] and that the neutralizing ability of antivenoms depends on the toxins they are directed towards.

The production of anticoral antivenoms is limited by the scarcity of *Micrurus* venoms. Their manufacture requires considerable quantities of the available venom for immunization procedures, but *Micrurus* species have small venom glands, producing low quantities of venom [18]. In theory, this difficulty could be resolved using many specimens. Still, *Micrurus* spp. have low survival in captivity due to low tolerance to changes in habitat and dietary preferences, which can lead to health problems [19]. Moreover, their terrestrial and semi-fossorial

habits and their relatively small size make it difficult to find them in the field [20, 21].

The expression of key toxins in heterologous organisms of easy manipulation, inexpensive, and rapid growth as *Escherichia coli* [22], have contributed to overcoming the scarcity of antigens while minimizing dependence on wild or captive individuals used for obtaining the quantities of venom needed to produce anticoral antivenoms. Thus, some of *Micrurus* venom proteins have been expressed in recombinant form and used as immunogens [23]. Clement et al. [24] expressed the neurotoxin Mlat1 from the coral snake *Micrurus laticorallus* in two different *E. coli* strains using the expression vector pQE30, and the recombinant Mlat1-produced rabbit polyclonal antibodies recognized native Mlat1. Guerrero-Garzón et al. [25] obtained four transcript sequences (MlatA1, B.D, B.E, D.H) from the venom glands of *M. diastema*, *M. laticollaris*, *M. browni*, and *M. tener*, which encoding type-I α -neurotoxins. Toxin D.H was identified in *M. diastema* venom and expressed in Origami Gold DE3 *E. coli* strain using pQE30. In addition, an anti-rD.H serum neutralized the neurotoxic effects of *M. diastema* native α -neurotoxins. Likewise, de la Rosa et al. [26] obtained ScNtx α -neurotoxins from the twelve most toxic short-chain α -neurotoxins sequences of elapid venom from *Acanthophis*, *Oxyuranus*, *Walterinnesia*, *Naja*, *Dendroaspis*, and *Micrurus* genera. These authors expressed a consensus sequence of ScNtx α -neurotoxins in *E. coli* Origami using the same pQE30 plasmid. The antibodies against ScNtx recognized short-chain α -neurotoxins of elapid venoms. Also, Liu et al. [27] obtained three recombinant 3FTxs proteins from three Asian cobra species (*Naja kaouthia*, *Naja atra*, *Naja siamensis*) using the pET-9a vector and an *E. coli* expression system. Immunization with each recombinant and a mixture of these (rsNTX, rLNTX, and rCTXA3) induced an immunological response to the native 3FTxs. Further, Ramos et al. [28] expressed recombinant multiepitope proteins in *E. coli* cells using the pAE vector. These authors developed an anti-elapid serum produced by a heterologous multiepitope DNA of most *M. coralinus* toxins. More recently, Romero-Giraldo et al. [29] expressed the most abundant PLA₂ from *M. dumerilii* in *E. coli* using the pET28a vector. The recombinant His-rMdumPLA₂ was biologically active, and anti-His-rMdumPLA₂ antibodies recognized its native homologous and the complete venom of *M. dumerilii*. Since Mipartoxin-1 is the most abundant toxin in *M. mipartitus* venom and one of the main causes of envenomings by this species, the main goal of this research was to produce the heterologous expression of this 3FTx and evaluate its immunogenic potential.

Methods

Bacterial strains, plasmids, and enzymes

Escherichia coli DH5 α (Invitrogen, Waltham, MA, USA) and BL21(DE3) (Stratagene, San Diego, CA, USA) strains were used for cloning and protein expression, respectively. Plasmid pET28a (Novogene, Cambridge, UK) was used as an episomal vector to deliver genetic construct to the *E. coli* BL21 (DE3) strain. New

England Biolabs (NEB) (Ipswich, MA, USA) NcoI, NotI, XhoI, EcoRV restriction enzymes, and T4 DNA ligase were used for the cloning process.

Plasmid construction

The synthetic expression construct of Mipartoxin-1 (UniProt: B3EWF8) from UniProt [30] was obtained by optimization of rare codons in *E. coli* using the codon database Kazusa [31] and the OPTIMIZER tool [32]. To verify the open reading frame, the *in-silico* translation of the optimized sequence was performed by the ExPASy tool [33]. A N-terminal polyhistidine tag (6HisTag), a glycine-serine linker, and the TEV proteolytic site were added to the target sequence. Two restriction sites allowed cloning of the construct in the episomal plasmid pET28a: the NcoI site was included at the 5' end and the NotI site at the 3' end after the termination codon. The synthetic construct was cloned into the pUC57_BsaI_Free vector, and the plasmid product was named HisrMipartoxin-1 (Figure 1A). The construct synthesis was carried out by General Biosystems.

Cloning HisrMipartoxin-1

Chimiocompetent *E. coli* DH5 α cells were transformed with the plasmid pUC57-rMipartoxin-1 or the empty pET28a vector by heat shock using the protocol described by Pope and Kent [34] with a modification in the heat-shocked time (40 sec). Transformed cells were recovered at 37 °C in Luria-Bertani broth (LB) for one hour and plated on LB plates that contained ampicillin (100 μ g/mL) or kanamycin (50 μ g/mL) as the selection antibiotic, respectively. Three individual colonies were grown overnight at 37 °C in 5 mL of LB medium supplemented with the respective antibiotic. The FavorPrep Plasmid Extraction Mini Kit (FAVORGEN Biotech Corporation, Wien, Austria) was used to isolate the plasmid DNAs contained in the *E. coli* strains, quantified with NanoDrop 2000 (Thermo Scientific, Waltham, MA, USA) and analyzed on 1% agarose gels stained with ethidium bromide. The plasmids and pET28a were cut with NcoI and NotI enzymes at 37 °C for three hours. The obtained fragments were gel-purified with the GeneJet Plasmid kit from Thermo Scientific (Waltham, MA, USA), ligated with T4 DNA ligase with a three-fold insert excess for two hours at room temperature, and finally transformed into chimiocompetent *E. coli* DH5 α cells. Transformed bacteria were incubated at 37 °C for 15 hours in selection LB media with kanamycin. Propagation and recovery were as above. Transformation confirmation and directionality of the insert were done by XhoI and EcoRV cutting and agarose gel analysis. XhoI cuts after position 1573, and EcoRV cuts after position 158 on pET28a.

Expression and purification of inclusion bodies

BL21(DE3) *E. coli* cells were transformed with the recombinant plasmid pET28a-HisrMipartoxin-1 by heat shock (as above), and then one single colony was selected in LB-Kanamycin (50 mg/mL) and used for pre-culture at 37 °C overnight.

HisrMipartoxin-1 expression and isolation from inclusion bodies were performed following the protocol described by Romero et al. [29]. In brief, 0.5 mM isopropyl-b-D-thiogalactopyranoside (IPTG) was added to the bacterial culture when it reached OD₆₀₀ nm between 0.6 and 0.7 while growing at 37°C until eight hours after induction. Biomass was harvested by centrifugation, washed with phosphate-buffered saline (PBS) buffer (pH 7.4), and resuspended in lysis buffer 100 mM Tris- 10 mM EDTA pH 8.5 for breaking the cells by sonication using an Ultrasonic Cell Disruptor (BIOBASE Biodustry, Shandong, China). The IBs were pelleted and dissolved at 16 h in equilibrium buffer (100 mM Tris- 10 mM EDTA- pH 8.0) in the presence of 8 M Urea and clarified by centrifugation. Refolding of HisrMipartoxin-1 was performed in dialysis tubing (SPECTRA / Por MWCO: 3.5 kDa) against a refolding buffer (200 mM Tris- 10 mM EDTA pH 8.5) with decreasing urea concentrations, starting 4 M up to 0.0625 M urea. Afterward, the recombinant solubilized protein was recovered by centrifuging at 32000 x g at 4 °C for 30 min.

Purification of HisrMipartoxin-1

The expressed HisrMipartoxin-1 protein was subjected to a two-step purification process: The first step consisted of a Ni-NTA (Ni-nitrilotriacetic acid) affinity chromatography using Ni-NTA agarose resin (Qiagen™ Ni-NTA Superflow) which was washed with the equilibrium buffer (this wash fraction was named 'flow-through'). Non-specific proteins and cellular debris were removed using two washes (W1 and W2) with 20 mM imidazole and 500 mM NaCl while elution (E) of the recombinant protein was achieved with 360 mM imidazole buffer. To cut the 6His-Tag, TEV protease (10 mg/mL) was used in the presence of a dialysis buffer [20 mM Tris pH 8.5, 100 mM NaCl, 5 mM 2-Mercaptoethanol (Sigma, Saint Louis, MO, USA)] and a SPECTRA/Por MWCO: 3.5 kDa tubing membrane. This cleavage was performed to confirm the approximate molecular mass of rMipartoxin-1, which is the recombinant protein without the tag. The second purification step was performed using a Prominence-20A chromatograph (Shimadzu, Kyoto, Japan). For this, it was used reverse-phase high-performance liquid chromatography (RP-HPLC) on a C18 column (250 X 10 mm, 5 μ m particle: Restek, Bellefonte, PA, USA). A linear gradient (0 to 70%) of an aqueous acetonitrile solution and 0.1% trifluoroacetic acid (TFA) at 1 mL/min for 35 min was applied. The elution signal was monitored at 215 nm with a photodiode detector (Shimadzu, Kyoto, Japan). Protein concentration (mg/mL) was determined using the Bradford protein assay [35].

SDS-PAGE and western blotting

Expression analysis of HisrMipartoxin-1 was assessed by SDS-PAGE in 14% Tris-tricine under reducing conditions according to Laemmli [36] and Schägger and von Jagow [37] protocols. Staining was made using Coomassie Brilliant Blue G-250 from Bio-Rad Laboratories (Hercules, CA, USA). A total of 10 μ g of the samples and 3 μ g of the molecular mass marker 11-250 kDa

from New England Biolabs (Ipswich, MA, USA) were loaded. Immunodetection of the recombinant protein was carried out following the protocol of Lomonte [38] with some adaptations. Briefly, samples from SDS-PAGE were electrotransferred to nitrocellulose membranes (0.45 mm) for one hour in a TRANS-BLOT SD system (BIO-RAD, California, USA) using transference buffer (192 mM Glycine- 25 mM Tris-10% Methanol pH 8.3). A blocking solution (1% BSA/Casein) and a washing solution (1:10 of the 1% BSA/Casein blocking solution) were used. In addition, an anti-Mipartoxin-1 (1:100) coupled to peroxidase obtained from rabbits inoculated with Mipartoxin-1 was used.

Mass spectrometry

The procedure for determining the molecular mass of the recombinant HisrMipartoxin-1 has been described in detail by Lomonte and Fernández [39] using a Q-Exactive Plus[®] Mass Spectrometer ESI-MS from Thermo Scientific (Waltham, MA, USA). Additionally, the monoisotopic masses were obtained by MS spectra deconvoluting with Freestyle[®] v.1.5 (Thermo Scientific, Waltham, MA, USA).

Venoms and animals

M. mipartitus venom (lyophilized) was obtained from adult specimens of both sexes collected by the Serpentarium of the University of Antioquia in the Antioquia region (Colombia). All *in vivo* experiments were performed using Swiss-Webster mice of both sexes of 18–20 g body weight. New Zealand female rabbits (1.7 kg) were utilized for *in vivo* immunization experiments. All experiments were performed following protocols approved by the ethics committee of the University of Antioquia (License No. 110 of 2017).

Lethal activity

Lethality induced by HisrMipartoxin-1 was evaluated following the protocol described by Cecchini et al. [40]. A group of four mice each received several doses up to 100 µg/mouse (6 µg/g body weight) in 300 µL of salt solution (SS) by the intraperitoneal (i.p.) route, while a control group received SS alone. The number of dead mice 24 hours after the injection was recorded.

Immunization and fractionation of anti-HisrMipartoxin-1 sera

Immunization with HisrMipartoxin-1 was performed following the protocol described in detail by Lomonte [38] with some adaptations such as the first dose of 277 µg and boost doses 416, 624, 936, 1404, 1404, 2106, and 2106 µg of the recombinant HisrMipartoxin-1 protein. For all boosts, IFA was used. Four bleedings were performed thus: before being immunized (pre-immune or 0-day) and at 29, 70, 112, and 169 days after the first immunization. Rabbit immunoglobulins were obtained by the caprylic acid (Sigma, Saint Louis, MO, USA) method described by Steinbuch and Audran [41] from rabbit blood collected during the bleeding. The sera and IgG concentrations were quantified in

a Nanodrop 2000 from Thermo Scientific (Waltham, MA, USA). Finally, sera were lyophilized and stored at -20 °C until used.

Antibodies titers and immunological recognition

The specific antibodies production against HisrMipartoxin-1 and immunological recognition of the specific rabbit sera were measured using an ELISA test following the protocol by Lomonte [38] with some modifications such as coating buffer (0.1 M Tris, 0.15 M NaCl pH 9.0) and washing buffer (PBS-0.05% Tween 20 pH 7.2). In short, 96 wells microplates (Falcon TM) were coated with 100 µL/well of 0.1 µg of venom *M. mipartitus* in coating buffer and incubated overnight at 4 °C. After, a blocking buffer (PBS-2% BSA) was added to wells for one hour and, subsequently, triplicate dilution curves of different sera and IgG were assayed separately (1:10, 1:100, 1:1000, 1:5000, and 1:10000). Two controls (serum pre-immune or non-immunized rabbit IgG was a negative control, and *M. mipartitus* venom was a positive control) were also included. After 1.5 h incubation, the plate was washed, and incubated with 100 µL of a dilution 1:8000 anti-rabbit IgG-peroxidase conjugate (Sigma, Saint Louis, MO, USA) for 1.5 h. After the last washing cycle was performed, the antibodies bound were observed by o-phenylenediamine (OPD), 2 mg/mL, and 30% H₂O₂. For absorbance readings, a Multiskan Sky Microplate Spectrophotometer from Thermo Scientific (Waltham, MA, USA) was used. The ELISA reaction was stopped by 0.32 M sulfuric acid. In another assay to evaluate cross-immunological recognition, HisrMipartoxin-1, Mipartoxin-1 [8], and Clarkitoxin-I-Mdum [9] were used to coat the plate, and the same procedure was followed as described.

Lethal effect neutralization by anti-HisrMipartoxin-1-IgG

To evaluate the neutralization ability of the immunoglobulins purified from anti-HisrMipartoxin-1 serum, several doses of anti-HisrMipartoxin-1-IgG were mixed with 1.5 LD₅₀ (13.5 µg/mouse) [42] of *M. mipartitus* venom or 1.5 LD₅₀ (9 µg/mouse) of Mipartoxin-1 [43], both in 300 µL of SS. These preparations were incubated for a half-hour at 37 °C and then injected by intraperitoneal (i.p.) route to three mice. The group that received the whole venom was used as a control, and observations were continued until 24 h after injection [44].

Statistical analysis

Results were expressed as the mean ± SD; a one-way ANOVA with Bonferroni post-test was used to determine significant differences (p < 0.05).

Results

HisrMipartoxin-1 cloning

The coding sequence of Mipartoxin-1 was optimized to *E. coli*-favored codons. The construction incorporated the cleavage sites NcoI, NotI, and XbaI. The first two were included for the

directional insertion into pET28a, while XbaI was added for future study. To conserve the open reading frame, a cytosine before the 6His-Tag was included, in addition to a proline and an alanine residue prior to the glycine-serine (GSGSGS) linker to confer flexibility to the histidine tail. Seven amino acids (ENLYFQG), corresponding to the cleavage site of the protease TEV, were included before the toxin sequence, and a UAG was included downstream of the target sequence. Cleavage of plasmid DNA and pET28a with NcoI and NotI endonucleases resulted in two fragments: one of the expected size (280 bp) and another of 5239 bp corresponding to pET28a (Figure 1A, B). The growth of transformed *E. coli* DH5 α colonies with the ligation product between the insert and pET28a was evidence of successful cloning. Transformed clones were confirmed by restriction analysis with XhoI and EcoRV yielding a fragment of 1578 bp and another fragment of 3958 bp (Figure 1B). The first fragment matched the insert (280 bp) expected size, plus a 1411 bp fragment (EcoRV-XhoI) without 113 bp released in cut, and the second fragment matched with a fragment spanning the XhoI-EcoRV segment.

Expression, purification, and lethal activity of HisrMipartoxin-1

The HisrMipartoxin-1 recombinant protein was expressed in *E. coli* strain BL21 (DE3) as a histidine hexamer-tagged (His-tag) fusion protein. HisrMipartoxin-1 was detected by SDS-PAGE (Figure 2A) as an insoluble protein (I) in inclusion bodies.

HisrMipartoxin-1 was subjected to *in vitro* folding and then recovered after two purification steps using agarose nickel affinity chromatography and further purification by RP-HPLC. After purification, the total yield of HisrMipartoxin-1 was 13.5 mg per liter of culture medium. The molecular mass of HisrMipartoxin-1 under reduced conditions after β -mercaptoethanol treatment was approximately 11 kDa (Figure 2A, arrow), close to the theoretical molecular mass (9887 Da). Furthermore, the molecular mass of HisrMipartoxin-1 determined by mass spectrometry was 9841 Da. As shown in Figure 2B, a gradual increase of expression of HisrMipartoxin-1 was evident as a band with a molecular mass of about 11 kDa, detected after two to eight hours of IPTG induction. The bacterial growth time to a density of 0.6-0.7 before induction with IPTG was considered as the initial time of 0 hours. The total-cell protein (T) content showed -besides HisrMipartoxin-1- several proteins of different molecular sizes with 0.5 mM IPTG induction. The insoluble (I) material resulting from cell lysate consisted of a thick band, and the soluble (S) fraction presented an electrophoretic profile different from the insoluble fraction, that is, no band was evident in the molecular mass detected in the insoluble fraction. Figure 2B shows the solubilized inclusion bodies (IBs) and the refolded HisrMipartoxin-1 protein (RP). The refolded HisrMipartoxin-1 was purified using nickel affinity chromatography. In all four fractions (flow-through, wash 1, wash 2, and elution), the presence of a band was noted of the expected molecular mass of HisrMipartoxin-1 (Figure 2B, arrow). The molecular mass of rMipartoxin-1 was confirmed after cutting

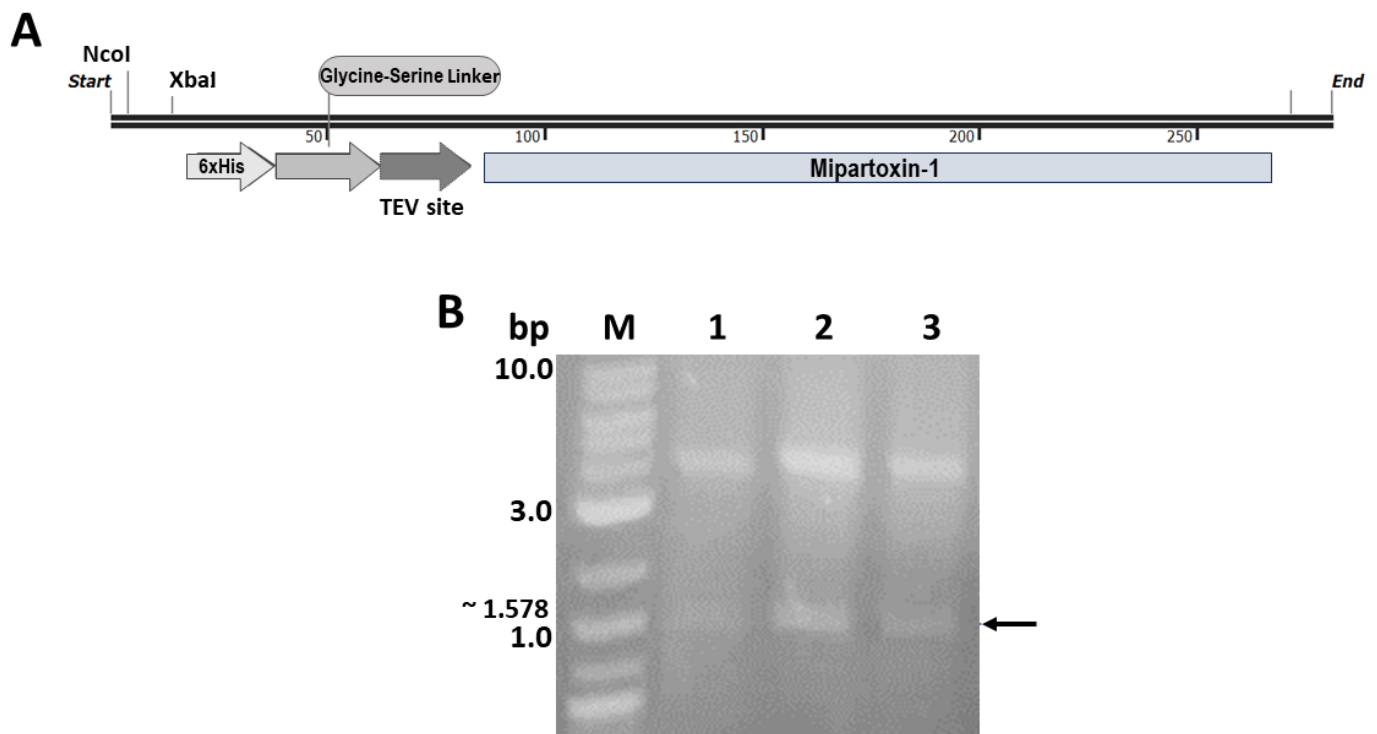


Figure 1. HisrMipartoxin-1 and digestion into pET28a. **(A)** Diagram of the genetic construction HisrMipartoxin-1. **(B)** Cleavage pET28a with XhoI and EcoRV on 1% agarose gel stained with ethidium bromide (Sigma, Saint Louis, MO, USA). MW: molecular weight marker (1 kb Plus DNA Ladder) (NEB); 1, 2, and 3: individual HisrMipartoxin-1 clones. The arrow indicates the 1578 bp expected fragment containing the 280 bp target insert.

the histidine tail. As shown in Figure 2C, a partial cut of the histidine tail was evident as two bands: a predominant band of the expected rMipartoxin-1 size (about 8 kDa), which was close to the reported molecular mass (~7 kDa) [8] and another band of about ~11 kDa corresponding to tagged HisrMipartoxin-1 protein. HisrMipartoxin-1 was also detected by western-blot assay (Figure 2D). Given that the tag cleavage was incomplete and the amounts of the recombinant protein that can be lost during the purification process decreased the total yield, we decided to continue using HisrMipartoxin-1 in all essays. Then, as a result of RP-HPLC purification, HisrMipartoxin-1 was identified at an elution time of about 16.0 min (Figure 3). To confirm the lethality of the purified toxin, both rMipartoxin-1 and HisrMipartoxin-1 were tested in mice. Neither caused

lethality in mice of 18-20 g of body weight (n = 4) in doses up to 100 µg/mouse.

Evaluation of anti-HisrMipartoxin-1 titers in serum

One rabbit was immunized with HisrMipartoxin-1 for six months, using a scheme that started with 277 µg of recombinant immunogen with an increase from 1.5 until the fifth immunization, one sustained dose in the sixth, followed by another increase from 1.5, and one final sustained dose in the eighth immunization. The serum samples of four bleedings were evaluated for their antibody levels against HisrMipartoxin-1. Results showed an increase of antibody titers against HisrMipartoxin-1 until 1:10000 (Figure 4). Differences were detected compared with the pre-immune serum ($p < 0.0001$).

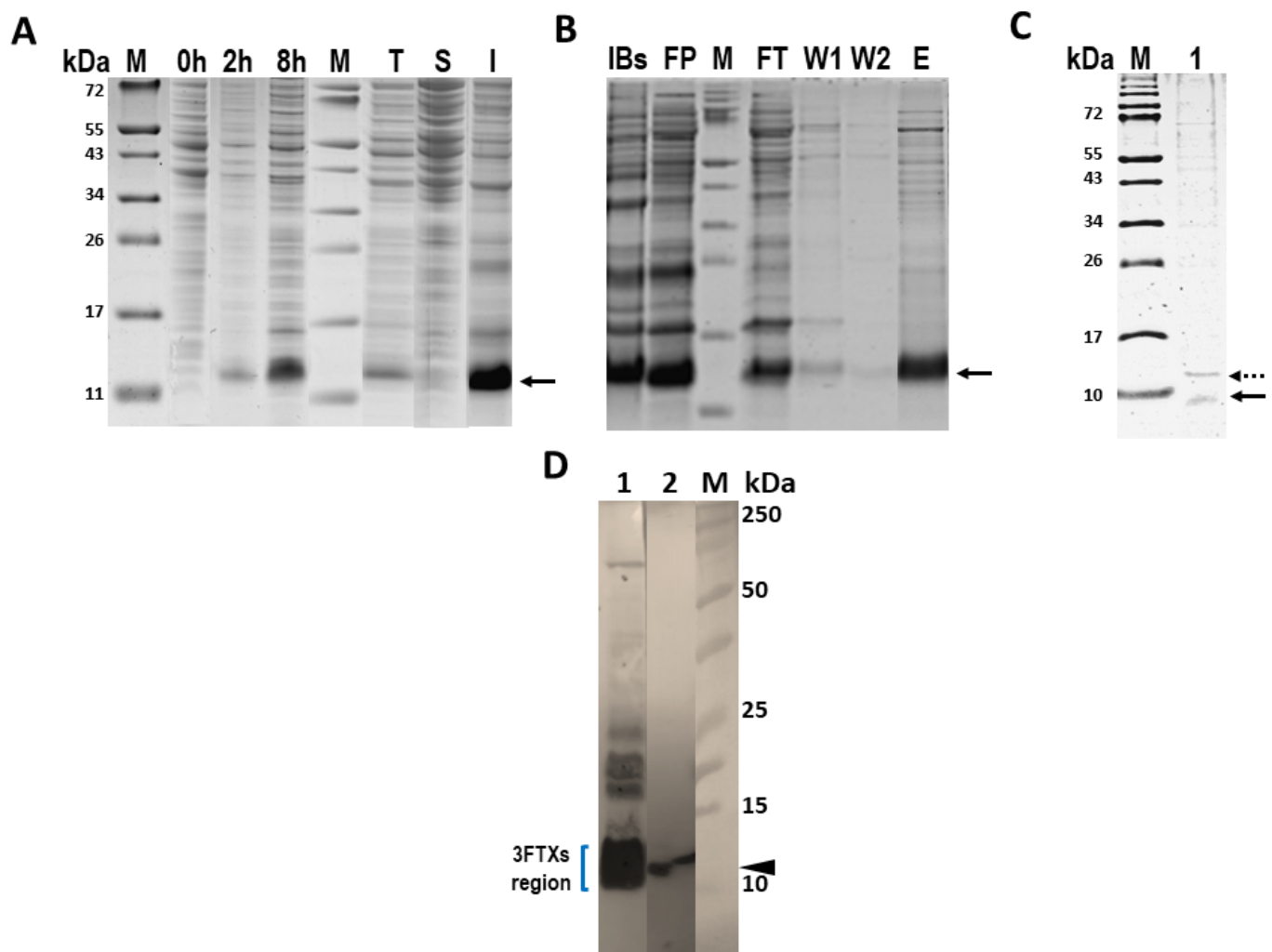


Figure 2. HisrMipartoxin-1 expressed in *E. coli* BL21 (DE3) strain. **(A)** SDS-PAGE analysis of HisrMipartoxin-1 before (at 0 hours) and after IPTG induction (at 2 and 8 hours). M: molecular mass marker; T: total protein; S: soluble fraction; I: insoluble fraction. **(B)** *In vitro* refolding and isolation of HisrMipartoxin-1. IBs: solubilized inclusion bodies; RP: refolded protein; FT: Flow-through; W1 and W2: Wash 1 and 2; E: Elution. **(C)** Cleavage of 6His-tag with TEV protease. rMipartoxin-1 was detected as a band of about 8 kDa (black arrow). HisrMipartoxin-1 showed approximately 11 kDa (dashed arrow). **(D)** Western blot analysis using the anti-Mipartoxin-1 antibody. Lane 1: The *M. mipartitus* venom profile contained different proteins; the region around 10 kDa is enriched in 3FTXs, particularly Mipartoxin-1 (7 kDa). The intensity of the band is due to their abundance in the *M. mipartitus* proteome. Lane 2: The molecular mass of HisrMipartoxin-1 was approximately 11 kDa (arrow). M: molecular mass marker in kDa.

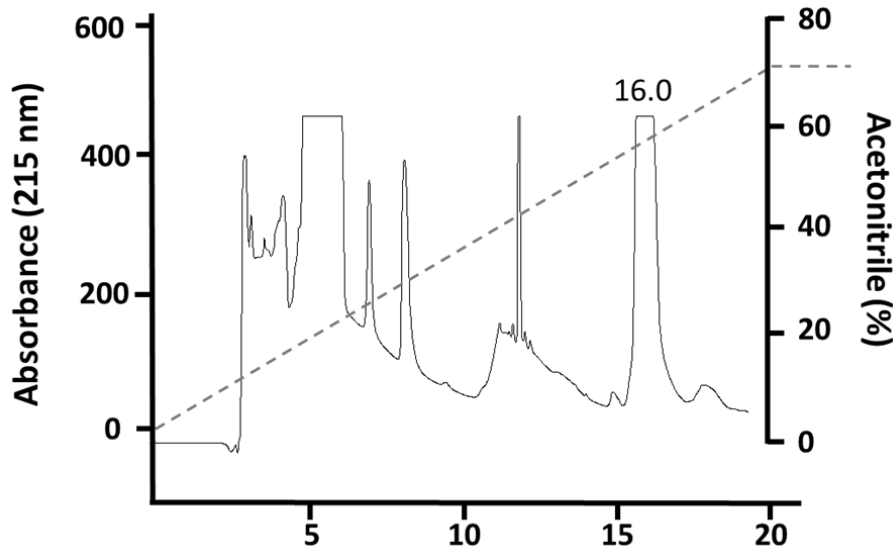


Figure 3. Purification by RP-HPLC chromatography. HisrMipartoxin-1 eluted at 16.0 min. An acetonitrile linear gradient and 1 mL/min flow were applied for elution.

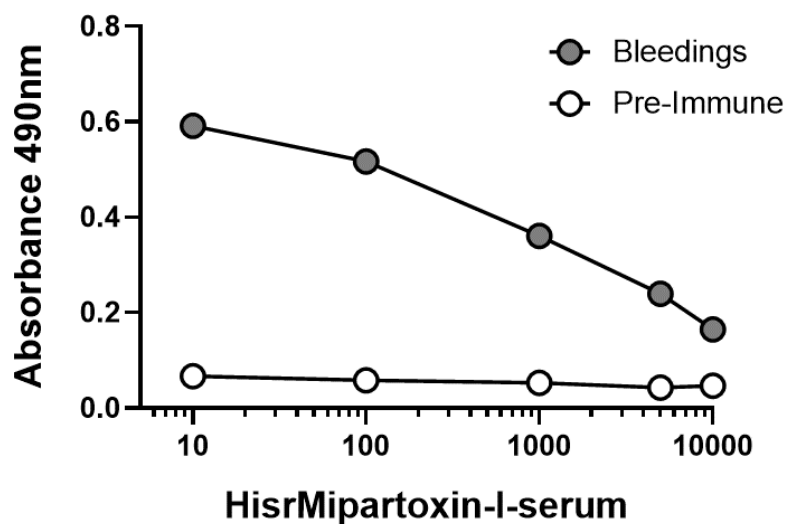


Figure 4. Antibody titers by ELISA in serum (average of four bleedings) against HisrMipartoxin-1. Sera from four bleedings in different dilutions (1:10 to 1:10000) were used, and absorbances were recorded at 490 nm. * Indicates differences with the pre-immune serum ($p < 0.0001$). Data correspond to the mean \pm SD ($n = 3$).

IgG purification, titers, and immunological cross-recognition

The fractionation of sera with caprylic acid allowed for obtaining IgG and reduction of albumin (Figure 5A). The anti-HisrMipartoxin-1-IgG yield was about 11.8 mg/mL. IgG was prepared at a concentration of ~ 50 mg/mL. Results showed an increase in IgG titers against HisrMipartoxin-1 from the first immunization (Figure 5B) and up to dilutions of 1:10000 (Figure 5C). Also, differences were detected in comparison to pre-immune IgG ($p < 0.0001$). Antibodies detected in serum and anti-HisrMipartoxin-1-IgG isolated showed reactivity

against its recombinant immunogen, and cross-reactions with Mipartoxin-1, *M. mipartitus* venom, and Clarkitoxin-I-Mdum were detected by ELISA (Figure 6).

Neutralization of the lethal effect of Mipartoxin-1 by anti-HisrMipartoxin-1-IgG

Anti-HisrMipartoxin-1-IgG neutralized 100% of the lethal effect of Mipartoxin-1, using a dose of 2 mg/mouse against 1.5 DI_{50} of native toxin (9 μ g). Lower doses did not inhibit the lethal effect. Additionally, anti-HisrMipartoxin-1-IgG did not neutralize the lethal effect of the *M. mipartitus* whole venom ($n = 3$) (results not shown).

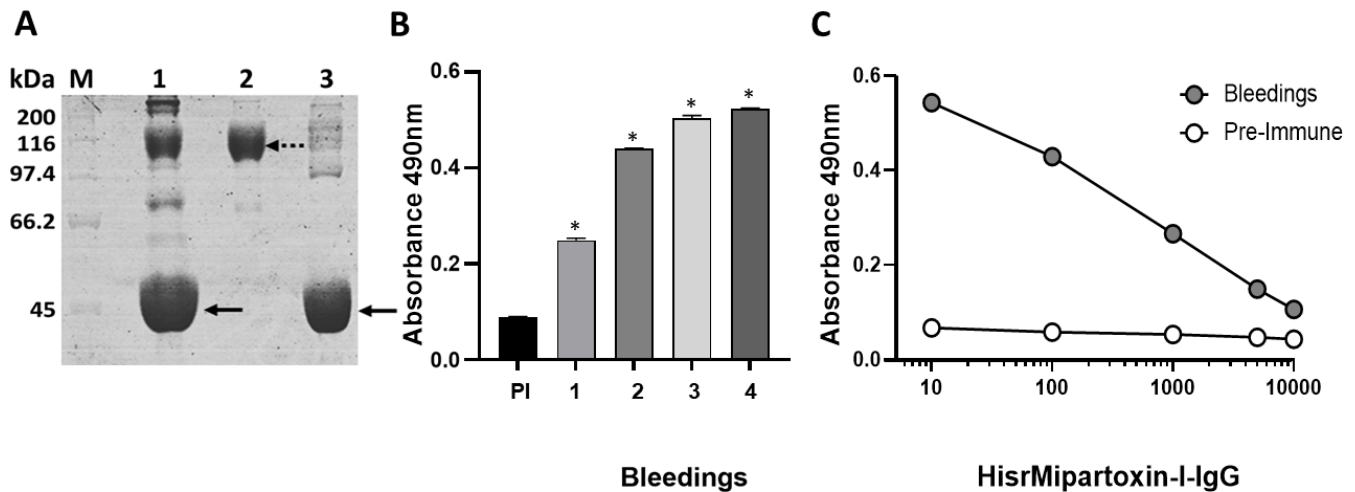


Figure 5. IgG purification, immunorecognition, and anti-HisrMipartoxin-1-IgG titers. **(A)** Fractionation IgG of hyperimmune serum using caprylic acid. Efficiency analysis was made by 10% SDS-PAGE under non-reducing conditions. The gels-stained with Coomassie Blue R-250. M: broad range molecular marker (kDa). 1: anti-HisrMipartoxin-1 serum; 2: IgG obtained after fractionation; 3: Albumin standard. The dashed arrow indicates the IgG band, and the black arrow indicates albumin. **(B)** Immunorecognition by ELISA of anti-HisrMipartoxin-1-IgG from each bleed (bleedings 1 to 4), and pre-immune serum (PI) against HisrMipartoxin-1. A 96-well plate was coated with HisrMipartoxin-1, and IgG from each bleeding was used at a 1:100 dilution (from an initial concentration of 50 mg/mL). The pre-immune serum was used at the same dilution. **(C)** Titration curve of anti-HisrMipartoxin-1-IgG by ELISA against HisrMipartoxin-1. IgG from four bleedings was used in dilutions from 1:10 to 1:10000 (from an initial concentration of 50 mg/mL). For B and C, * indicates differences compared to the pre-immune serum ($p < 0.0001$). Data correspond to the mean \pm SD ($n = 3$).

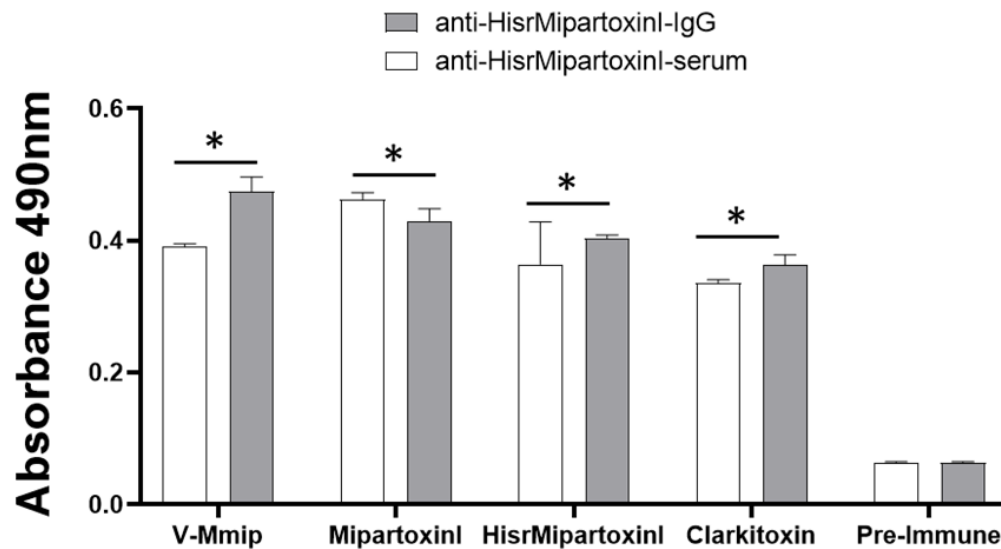


Figure 6. Immunoreactivity by ELISA of sera and IgG anti-HisrMipartoxin-1 against *M. mipartitus* venom (V-Mmip), Mipartoxin-1 (native), HisrMipartoxin-1, and Clarkitoxin-I-Mdm. *Indicates differences when compared to the pre-immune serum ($p < 0.0001$). Data correspond to the mean \pm SD ($n = 3$).

Discussion

Owing to the scarcity of *Micrurus* venoms, investigations have focused on the biochemical and pharmacological properties of whole venoms and the properties of isolated toxins. However, in recent years, biotechnological developments and improved chromatographic methods have greatly simplified the expression and purification of recombinant toxins from some species of *Micrurus* intending to improve antivenom production and solve, in part, the venom scarcity.

In general, snake venoms are a cocktail of pharmacologically active proteins and peptide components that can be enzymatic or nonenzymatic [45]. Most of these components are immunogenic (~98% of their dry weight), including toxins that induce both severe and non-toxic effects [46]. One of the most important toxin families in elapid venoms are the 3FTxs, neurotoxins whose primary target is the peripheral nervous system and cause neuromuscular weakness and paralysis [47]. The most abundant 3FTx (Mipartoxin-1) of *M. mipartitus* venom was

isolated and sequenced by Rey-Suarez et al. [8]. Mipartoxin-1 is lethal and causes neurotoxic effects [8]. Cardona-Ruda et al. [43] recently demonstrated that antibodies produced against Mipartoxin-1 (Mm8) and MmipPLA₂ (Mm20) neutralize *M. mipartitus* whole venom. This work presents the production of recombinant Mipartoxin-1 and its immunogenic potential.

Mipartoxin-1 was produced in an expression plasmid encoding a synthetic gene codon optimized for *E. coli*. The construct HisrMipartoxin-1 overexpressed the target protein in *E. coli* BL21 (DE3), and its yield was 13.5 mg/L after purification. Protein yields in the range of 10–50 mg/L correspond to medium-level expression for recombinant proteins, as has been reported [48, 49]. It is important to stress that *E. coli* strains differentially express heterologous genes, and intrinsic features of the pET vector can also be a determining factor for achieving different expression levels of the recombinant proteins [50]. The yield (13.5 mg/L) of HisrMipartoxin-1 after purification is comparable with yields obtained for a different type of snake venom protein such as PLA₂s: for instance, Romero-Giraldo et al. [29] obtained a yield of 10.1 mg/L for His-rMdumPLA₂, a PLA₂ from *M. dumerilii* expressed in the BL21 (DE3) strain from *E. coli* using pET28a as the expression vector.

Several authors have reported yields for other recombinant 3FTXs from different species [22–23, 51–53] and other low molecular weight toxins such as PLA₂s [54], which vary according to the *E. coli* strain, the plasmid vector, and expression conditions. In this context, it has been posed that recombinant protein yields may be associated with several factors, such as the growth rate of the host cells and the absolute amount of soluble protein produced per culture volume [55], the His-tag that confers stability to the protein [56], the vector backbone and design and the cloning strategy [29, 57].

The mass of HisrMipartoxin-1 detected by SDS-PAGE is close to its theoretical molecular mass (9887 Da), however, it differed from the native Mipartoxin-1, which has a molecular mass of 7030 Da [8]. The difference between the deduced molecular mass and the SDS-PAGE mobility for HisrMipartoxin-1 is a consequence of the elements included in the genetic construct, such as the histidine segment, the linker GS, and the TEV protease sequence. The rMipartoxin-1 molecular mass after the tag cleavage was comparable to the native toxin (Mipartoxin-1), evidenced in the TEV protease cleavage assay.

HisrMipartoxin-1 was expressed as IBs, hence it had to be solubilized with a denaturing agent, such as urea. However, in contrast to the native protein, solubilization of the HisrMipartoxin-1 IBs did not result in a protein with biological activity [8]. This result is due to non-native intermolecular and intramolecular interactions during the refolding process [58], which may produce misfolding or incomplete protein folding [59, 60] with the formation of non-native disulfide bonds [61], which together generate a non-native protein. It should be noted that the cysteine pattern is a highly conserved feature among 3FTXs [62], just like Tyr25 and Phe27 residues, which play a key role in correct folding [63]. Therefore, any change

in the primary structure may affect biological functions and the molecular targets [64]. On the other hand, considering that the activity of the protein is closely correlated to its native structure [65, 66], another possible explanation is that although the presence of the His-tag confers stability to recombinant protein [56], also may cause negative effects on the tertiary structure during the refolding process, altering target and/or inhibitor interaction sites or the biological activity of the protein [67], a subject that warrants further study. Nonetheless, it is documented that the insertion of sequences in protein structures may decrease conformational stability and cause the loss or reduction of biological activity [68]. In addition, impurities that result during the solubilization process of IBs can interact with the expressed protein and interfere with its proper folding [58].

Moreover, it is important to note that the percent active protein recovered during *in vitro* refolding is less than 50% [69], and in other cases, no biologically active protein is obtained [70]. Taken together, HisrMipartoxin-1 adopted a stable soluble conformation, but its crucial fold -typical of the 3FTXs- consisting of three β -sheet loops with all four conserved disulfide bridges [62] may not have been obtained, therefore lethal activity was not observed. In fact, Girish and colleagues [71] have suggested that the biological activities of 3FTXs might be associated with slight conformational differences in the three β -sheet loops, inferring that a small change in the protein structure could alter its functionality. However, confirmation of this hypothesis needs further studies.

Western-blot analysis showed that the native Mipartoxin-1 antiserum recognized HisrMipartoxin-1. Similarly, this antiserum recognized the 3FTXs region present in *M. mipartitus* venom. Additionally, rabbit polyclonal antibodies generated against HisrMipartoxin-1 recognized *M. mipartitus* venom, native Mipartoxin-1, and Clarkitoxin-I-Mdum from *M. dumerilii*. It is possible that some antigenic determinants were recognized by the anti-HisrMipartoxin-1 antibodies, which were generated because of the rabbit immune response. In addition, considering that *Micrurus* antivenoms have variable immunological cross-reactivity according to different authors [72–76] and a cysteine pattern of the short-chain 3FTXs (or “type-I”) [77] conserved in many elapid venoms [9], the immunological cross recognition of antibodies against HisrMipartoxin-1 might be a consequence of a conserved backbone of both native toxins. While it is true that the Clarkitoxin-I-Mdum and Mipartoxin-1 sequences share only 26% identity between amino acid sequences [9], this study shows that the possible structural changes of the recombinant protein favored some conserved antigenic determinants resulting in the cross-recognition against 3FTX other than Mipartoxin-1. In addition, this result contrasts with the study from Rey-Suárez et al. [9], who reported that the anti-Mipartoxin-I or anti-Clarkitoxin-I-Mdum sera recognized components in *M. mipartitus* and *M. clarki* venoms, but did not cross-recognize their homologous antigen, Mipartoxin-1, and Clarkitoxin-I-Mdum, respectively.

Our results showed that the immune response was evident by the presence of antibodies against HisrMipartoxin-1 from the first immunization, indicating that the recombinant immunogen generated an immunological response. Although antibody titers were low, it is known that 3FTxs, being low molecular mass proteins, generate a low immune response [38, 78–79]. Proof of this is the results obtained by Laustsen et al. [80], Fernández et al. [81], and Cardona-Ruda et al. [43], who showed that 3FTxs induced a lower immune response compared to the PLA₂s. Nevertheless, these groups of toxins are responsible for the most important toxic effects observed in coral snakebite victims [5, 14]. Further, HisrMipartoxin-1 did not induce toxic effects, which could be an advantage since it reduces the possibility of inducing toxicity during the immunization process.

Additionally, it was found that anti-HisrMipartoxin-1-IgG completely neutralized the lethal effect of the native Mipartoxin-1. Toxin neutralization has been considered to take place when the antibody is bound by the variable region [80]. It is possible to hypothesize that some epitopes are located on conserved structures, specifically on loop II of the 3FTx, as has been reported [22, 82]. However, this hypothesis needs to be proved in further studies. It has also been reported that recombinant proteins from IBs produce neutralizing antibodies [83]. In contrast, although the antibodies did not neutralize the *M. mipartitus* whole venom, these were highly recognized in the whole venom. This is because another lethal component has been reported named MmipPLA₂ (LD₅₀ 0.85 µg/mouse [7]), the most abundant PLA₂ from *M. mipartitus* venom. Also, as mentioned above, similar findings were reported by Cardona-Ruda et al. [43], who used IgG against the native toxin and demonstrated that the MmipPLA₂ toxin was involved in the lethal effect and that the lethal effect of the venom was neutralized only with a mixture of antibodies against these two toxins (Mipartoxin-1 and MmipPLA₂) [7, 43]. Given that HisrMipartoxin-1 generated non-neutralizing antibodies against venom *M. mipartitus*, uncover the need to include other key toxins of *M. mipartitus*, in the production of anti-*Micrurus* antivenoms to improve the neutralizing ability against this species.

Consistent with the findings above and considering that neutralization of single toxins by antibodies may notably reduce the clinical manifestations of envenoming given their high toxicity and high abundance in the venom [80, 84], the development of recombinant proteins containing epitopes from the main toxic components from *M. mipartitus* venom could be a powerful source of key antigens for the preparation of neutralizing antibodies [85]. Likewise, it is important to highlight that immunization with a snake venoms mixture [86, 87] or a mixture of their main toxins [88] increases the neutralization scope of the antivenom. In this sense, mixtures of antibodies against key toxins can result in an efficient strategy to neutralize most of the medically relevant snake venom toxins [27, 84, 89–992].

Ultimately, this work demonstrates that HisrMipartoxin-1 induces antibodies in an animal model with the neutralization ability of Mipartoxin-1, one of the toxins responsible for the lethal effect of *M. mipartitus* venom. Thus, this recombinant toxin can be used as an immunogen to improve the development of an anticoral antivenom and overcome the limitations associated with the availability of *M. mipartitus* venom.

Conclusion

In this study, the heterologous expression of HisrMipartoxin-1, the most abundant 3FTx of *M. mipartitus* venom (Mipartoxin-1), was achieved using *E. coli* BL21 (DE3). This work is the first report of a recombinant 3FTx from *M. mipartitus* venom. HisrMipartoxin-1 induced antibodies that neutralized the lethal effect of the native toxin. These results advance the development of anticoral antivenom using recombinant toxins and offer a solution to the limited access and limitations in the availability of venom from *Micrurus* species.

Abbreviations

BP: base pairs; BSA: Bovine serum albumin; EDTA: Ethylenediaminetetraacetic acid; ELISA: Enzyme-Linked Immunosorbent Assay; GS: Glycine Serine; IB: Inclusion body; IFA: Incomplete Freund's adjuvant; INS: Instituto Nacional de Salud; i.p.: Intraperitoneal route; IPTG: isopropyl-β-D-thiogalactopyranoside; kDa: Kilodalton; LD: Lethal dose; LB: Luria-Bertani broth; MWCO: molecular-weight cutoffs; Ni-NTA: Ni-nitrilotriacetic acid; nm: nanometer; OPD: o-phenylenediamine; PBS: phosphate-buffered saline; PLA₂: Phospholipase A₂; RP-HPLC: Reversed Phase-High-performance liquid chromatography; SD: Standard deviation; SDS-PAGE: Sodium dodecyl-sulfate polyacrylamide gel electrophoresis; SS: Salt solution; TFA: Trifluoroacetic acid; WHO: World Health Organization; 3FTx: three finger toxins.

Acknowledgments

The authors thank Dr. Daniela Seelenfreund for the English grammar edition. We greatly appreciate the technical support from Jorge Asprilla is very much acknowledged and the Serpentarium of the University of Antioquia team.

Availability of data and materials

The datasets generated during and/or analyzed during the current study are available from the corresponding author upon reasonable request.

Funding

This research was funded by Ministerio de Ciencia, Tecnología e Innovación- MinCiencias (grant number 57474), and the University of Antioquia (UdeA) for partial financial support for this study.

Competing interests

The authors have declared that no conflicts of interest exist regarding this manuscript.

Authors' contributions

Conception of the work, SP., PR-S., and VN; Collection of data: LER-G, SP, PR-S, and VN; Analysis of data, LER-G, SP, PR-S, and VN; Funding acquisition, JAP; Investigation, LER-G, SP, PR-S, VN, MS-C, and JAP; Methodology, LER-G, MAB, MFF, PR-S, and VN; Resources, SP, and JAP; Supervision, VN and JAP; Writing of manuscript, LER-G, SP, PR.-S., VN, and JAP; Writing—review and editing, LER-G, PR-S, VN, MS-C, and JAP. All authors have read and agreed to the published version of the manuscript.

Ethics approval

This study had authorization from the Ministry of Environment to access genetic resources (RGE: 0156–9, 15 August 2018).

Consent for publication

Not applicable.

References

- World Health Assembly. Addressing the Burden of Snakebite Envenoming. 2018 Sep 12;17.
- Gutiérrez JM, Calvete JJ, Habib AG, Harrison RA, Williams DJ, Warrell DA. Snakebite envenoming. *Nat Rev Dis Primers*. 2017 Sep 14;3:17063.
- Instituto Nacional de Salud. Portal SIVIGILA. Accidente Ofídico. Período Epidemiológico XIII-2022. Colombia.
- Roze JA. Coral Snakes of the Americas: Biology, Identification, and Venoms; Krieger Publishing Company (Malabar, FL, United States); 1996.
- Otero-Patiño R. Snake Bites in Colombia. In: Gopalakrishnakone P, Faiz SMA, Gnanathanan CA, Habib AG, Fernando R, Yang C-C, editors. *Clinical Toxinology*. Dordrecht, The Netherlands: Springer; 2014. p.1-42.
- Lomonte B, Rey-Suárez P, Fernández J, Sasa M, Pla D, Vargas N, Bénard-Valle M, Sanz L, Corrêa-Netto C, Núñez V, Alape-Girón A, Alagón A, Gutiérrez JM, Calvete JJ. Venoms of *Micrurus* coral snakes: Evolutionary trends in compositional patterns emerging from proteomic analyses. *Toxicon*. 2016 Nov;122:7-25.
- Rey-Suárez P, Núñez V, Gutiérrez JM, Lomonte B. Proteomic and biological characterization of the venom of the redbellied coral snake, *Micrurus mipartitus* (Elapidae), from Colombia and Costa Rica. *J. Proteom*. 2011;75(2):655–67.
- Rey-Suárez P, Floriano RS, Rostelato-Ferreira S, Saldarriaga-Córdoba M, Núñez V, Rodrigues-Simioni L, Lomonte B. Mipartoxin-1, a novel three-finger toxin, is the major neurotoxic component in the venom of the redbellied coral snake *Micrurus mipartitus* (Elapidae). *Toxicon*. 2012;60(5):851–63.
- Rey-Suárez P, Saldarriaga-Córdoba M, Torres U, Marin-Villa M, Lomonte B, Núñez V. Novel three-finger toxins from *Micrurus dumerilii* and *Micrurus mipartitus* coral snake venoms: Phylogenetic relationships and characterization of Clarkitoxin-I-Mdum. *Toxicon*. 2019 Dec;170: 85–93.
- De Abreu VA, Leite GB, Oliveira CB, Hyslop S, Furtado MFD, Simioni LR. Neurotoxicity of *Micrurus altirostris* (Uruguayan coral snake) venom and its neutralization by commercial coral snake antivenom and specific antiserum raised in rabbits. *Clin Toxicol (Phila)*. 2008;46(6):519–27.
- Camargo TM, de Roodt AR, da Cruz-Höfling MA, Rodrigues-Simioni L. The neuromuscular activity of *Micrurus pyrrhocryptus* venom and its neutralization by commercial and specific coral snake antivenoms. *J Venom Res*. 2011;2:24–31.
- Pérez ML, Fox K, Schaer M. A retrospective evaluation of coral snake envenomation in dogs and cats: 20 cases (1996-2011). *J Vet Emerg Crit Care*. 2012;22(6):682–9.
- Wood A, Schauben J, Thundiyil J, Kunisaki T, Sollee D, Lewis-Younger C, Bernstein J, Weisman R. Review of Eastern coral snake (*Micrurus fulvius fulvius*) exposures managed by the Florida Poison Information Center Network: 1998-2010. *Clin Toxicol (Phila)*. 2013;51(8):783-8.
- Bucarety F, Capitani EM, Vieira RJ, Rodrigues CK, Zannin M, Da Silva NJ Jr, Casais-e-Silva LL, Hyslop S. Coral snake bites (*Micrurus* spp.) in Brazil: a review of literature reports. *Clin Toxicol (Phila)*. 2016;54(3):222-34.
- Instituto Nacional de Salud. Inserto Suero Antiofídico Polivalente. 2017, Colombia [cited 2023 April 10]. Available from: <https://www.ins.gov.co/Direcciones/Produccion/Paginas/Suero-antiofídico-polivalente.aspx>.
- Rey-Suarez P, Lomonte B. Immunological cross-recognition and neutralization studies of *Micrurus mipartitus* and *Micrurus dumerilii* venoms by two therapeutic equine antivenoms. *Biologicals*. 2020;68:40e45.
- Piedrahita JD, Cardona-Ruda A, Pereañez JA, Rey-Suárez P. In-depth immunorecognition and neutralization analyses of *Micrurus mipartitus* and *M. dumerilii* venoms and toxins by a commercial antivenom. *Biochimie*. 2024;216:120-5.
- de Roodt AR, Dolab JA, Galarce PP, Gould E, Litwin S, Dokmetjian JC, Segre L, Vidal JC. A study on the venom yield of venomous snake species from Argentina. *Toxicon*. 1998;36(12):1949–57.
- Travaglia S, Gomes A, Puerto G. Maintenance and reproductive behavior of *Micrurus corallinus* in captivity. In: da Silva J, Porras W, Aird S, da Costa A. editors. *Advances in coral snake biology: with an emphasis on South America*. LC, Utah, United States: Eagle Mountain Publishing; 2021. p. 353-69.
- Henao-Duque AM, Núñez V. Maintenance of red-tail coral snake (*Micrurus mipartitus*) in captivity and evaluation of individual venom variability. *Acta Biol Colomb*. 2016;21(3):593-600.
- Mendes GF, Stuginski DR, Loibel SMC, Morais-Zani K, da Rocha MMT, Fernandes W, Sant'Anna SS, Grego KF. Factors that can influence the survival rates of coral snakes (*Micrurus corallinus*) for antivenom production. *J Anim Sci*. 2019;97(2):972-80.
- Tasoulis T, Isbister G. A review and database of snake venom proteomes. *Toxins (Basel)*. 2017;9(9):290.
- Lomonte B, Calvete J, Fernández J, Pla D, Rey-Suárez P, Sanz L, Gutiérrez J, Sasa M. Venomic analyses of coral snakes. In: da Silva J, Porras W, Aird S, da Costa A, editors. *Advances in coral snake biology: with an emphasis on South America*. LC, Utah, United States: Eagle Mountain Publishing; 2021. p. 485-518.
- Clement H, Flores V, De la Rosa G, Zamudio F, Alagon A, Corzo G. Heterologous expression, protein folding and antibody recognition of a neurotoxin from the Mexican coral snake *Micrurus laticorallus*. *J Venom Anim Toxins incl Trop Dis*. 2016;22:25. doi: 10.1186/s40409-016-0080-9.
- Guerrero-Garzon J, Bénard-Valle B, Restano-Cassulini R, Zamudio F, Corzo G, Alagon A, Olvera-Rodríguez A. Cloning and sequencing of three-finger toxins from the venom glands of four *Micrurus* species from Mexico and heterologous expression of an alpha-neurotoxin from *Micrurus diastema*. *Biochimie*. 2018;147:114–21.
- de la Rosa G, Corrales-García L, Rodríguez-Ruiz X, López-Vera E, Corzo G. Short-chain consensus alpha-neurotoxin: A synthetic 60-mer peptide with generic traits and enhanced immunogenic properties. *Amino Acids*. 2018;50(7):885–95.
- Liu BS, Jiang BR, Hu KC, Liu CH, Hsieh WC, Lin MH, Sung WC. Development of a Broad-Spectrum Antiserum against Cobra Venoms Using Recombinant Three-Finger Toxins. *Toxins*. 2021;13(8):556.
- Ramos H, Junqueira-de-Azevedo I, Novo J, Castro K, Duarte C, Machado-de-Ávila R, Chavez-Olortegui C, Ho PL. A Heterologous Multi-epitope DNA Prime/Recombinant Protein Boost Immunisation Strategy for the Development of an Antiserum against *Micrurus corallinus* (Coral Snake) Venom. *PLoS Negl Trop Dis*. 2016;10(3):e0004484.
- Romero-Giraldo LE, Pulido S, Berrío MA, Flórez MF, Rey-Suárez P, Núñez V, Pereañez JA. Heterologous Expression and Immunogenic Potential of the Most Abundant Phospholipase A₂ from Coral Snake *Micrurus dumerilii* to Develop Antivenoms. *Toxins*. 2022;14(12):825.

30. UniProt: the universal protein knowledgebase in 2021. The UniProt Consortium. *Nucleic Acids Research*. 2021 Jan 8;49(D1):D480–9.
31. Nakamura Y, Gojobori T, Ikemura T. Codon usage tabulated from the international DNA sequence databases: status for the year 2000. *Nucleic Acids Res*. 2000 Jan 1;28(1):292.
32. Puigbo P, Guzman E, Romeu A, Garcia-Valle S. Optimizer: A web server for optimizing the codon usage of DNA sequences. *Nucleic Acids Res*. 2007 Jul;35:W126–31.
33. Séverine Duvaud, Chiara Gabella, Frédérique Lisacek, Heinz Stockinger, Vassilios Ioannidis, Christine Durinx. ExPasy, the Swiss Bioinformatics Resource Portal, as designed by its users. *Nucleic Acids Res*. 2021 Jul 2;49(W1):W216–27.
34. Pope B, Kent HM. High Efficiency 5 Min Transformation of *Escherichia coli*. *Nucleic Acids Res*. 1996;24(3):536–7.
35. Bradford MM. A rapid and sensitive method for the quantitation of microgram quantities of protein utilizing the principle of protein-dye binding. *Anal. Biochem*. 1976;72:248–54.
36. Laemmli UK. Cleavage of structural proteins during the assembly of the head of bacteriophage T4. *Nature*. 1974;22(5259):680–5.
37. Schägger H, von Jagow G. Tricine-sodium dodecyl sulfate-polyacrylamide gel electrophoresis for the separation of proteins in the range from 1 to 100 kDa. *Analytical Biochemistry*. 1987;166:368–79.
38. Lomonte B. *Manual de Métodos Inmunológicos*. Univ Costa Rica. 2007.
39. Lomonte B, Fernández J. Solving the microheterogeneity of *Bothrops asper* myotoxin-II by high-resolution mass spectrometry: Insights into C-terminal region variability in Lys49-phospholipase A2 homologs. *Toxicon*. 2022;210:123–31.
40. Cecchini AL, Marcussi S, Silveira LB, Borja-Oliveira CR, Rodrigues-Simioni L, Amara S, Stábeli RG, Giglio JR, Arantes EC, Soares AM. Biological and enzymatic activities of *Micrurus* sp. (Coral) snake venoms. *Comp Biochem Physiol A: Mol Integr Physiol*. 2005;140(1):125–34.
41. Steinbuch M, Audran R. Isolation of IgG immunoglobulin from human plasma using caprylic acid. *Rev Fr Etud Clin Biol*. 1969;14(10):1054–8.
42. Otero R, Osorio RG, Valderrama R, Giraldo CA. Efectos farmacológicos y enzimáticos de los venenos de serpientes de Antioquia y Chocó (Colombia). *Toxicon*. 1992;30:611–20.
43. Cardona-Ruda A, Rey-Suárez P, Núñez V. Anti-Neurotoxins from *Micrurus mipartitus* in the Development of Coral Snake Antivenoms. *Toxins*. 2022;14(4):265.
44. Gutiérrez JM, Solano G, Pla D, Herrera M, Segura A, Vargas M, León G. Preclinical evaluation of the efficacy of antivenoms for snakebite envenoming: state-of-the-art and challenges ahead. *Toxins*. 2017;9(5):163.
45. Pahari S, Bickford D, Fry BG, Kini RM. Expression pattern of three-finger toxin and phospholipase A₂ genes in the venom glands of two sea snakes, *Lapemis curtus* and *Acalyptophis peronii*: comparison of evolution of these toxins in land snakes, sea kraits and sea snakes. *BMC Evolutionary Biology*. 2007 Sep 27;7(175).
46. León G, Sánchez L, Hernández A, Villalta M, Herrera M, Segura A, Estrada R, Gutiérrez JM. Immune response towards snake venoms. *Inflamm Allergy Drug Targets*. 2011;10(5):381–98.
47. Waheed H, Moin SF, Choudhary MI. Snake Venom: From Deadly Toxins to Life-saving Therapeutics. *Curr Med Chem*. 2017;24(17):1874–91.
48. Rudolph R, Lilie H. *In vitro* folding of inclusion body proteins. *FASEB J*. 1996;10(1):49–56.
49. Packiam KAR, Ooi CW, Li F, Mei S, Tey BT, Ong HF, Song J, Ramanan RN. Periscope-Opt: Machine learning-based prediction of optimal fermentation conditions and yields of recombinant periplasmic protein expressed in *Escherichia coli*. *Comput Struct Biotechnol J*. 2022;20:2909–20.
50. Rosano G, Ceccarelli E. Recombinant protein expression in *Escherichia coli*: Advances and challenges. *Front Microbiol*. 2014 Jul 8;5:341.
51. Shulepko MA, Lyukmanova EN, Shenkarev ZO, Dubovskii PV, Astapova MV, Feofanov AV, Arseniev AS, Utkin YN, Kirpichnikov MP, Dolgikh DA. Towards universal approach for bacterial production of three-finger Ly6/uPAR proteins: Case study of cytotoxin I from cobra *N. oxiana*. *Protein Expr Purif*. 2017 Feb;130:13–20.
52. Xu J, Li J, Wub X, Song C, Lin Y, Shen Y, Ye W, Sun C, Wanga X, Li Z, Liu Y, Wei L, Li Z, Xu Z. Expression and refolding of bioactive a-bungarotoxin V31 in *E. coli*. *Protein Expr Purif*. 2015;110:30–6.
53. Bénard-Valle M, Neri-Castro E, Elizalde-Morales N, Olvera-Rodríguez A, Strickland J, Acosta G, Alagón A. Protein composition and biochemical characterization of venom from Sonoran Coral Snakes (*Micrurus euryxanthus*). *Biochimie*. 2021;182:206–16.
54. Yang WL, Peng LS, Zhong XF, Wei JW, Jiang XY, Ye LT, Zou L, Tu HB, Wu WY, Xu AL. Functional expression and characterization of a recombinant phospholipase A2 from sea snake *Lapemis hardwickii* as a soluble protein in *E. coli*. *Toxicon*. 2003;41(6):713–21.
55. Woestenenk E, Hammarström M, Van den Berg S, Härd T, Berghind H. His tag effect on solubility of human proteins produced in *Escherichia coli*: A comparison between four expression vectors. *J Struct Funct Genom*. 2004;5(3):217–29.
56. Mohanty A, Wiener M. Membrane protein expression and purification: Effects of polyhistidine tag length and position. *Protein Expr Purif*. 2004;33(2):311–25.
57. de Marco A. Recombinant polypeptide production in *E. coli*: towards a rational approach to improve the yields of functional proteins. *Microb Cell Fact*. 2013;12:101.
58. Bhavesh N, Panchal S, Mittal R, Hosur R. NMR identification of local structure preferences IHIV protease tethered heterodimer in 6M guanidine hydrochloride, *FEBS Lett*. 2001;509(2):218–24.
59. Gonzalez-Montalban N, Garcia-Fruitos E, Villaverde A. Recombinant protein solubility-does more mean better? *Nat Biotechnol*. 2007;25(7):718–20.
60. Martinez-Alonso M, Gonzalez-Montalban N, Garcia-Fruitos E, Villaverde A. The functional quality of soluble recombinant polypeptides produced in *Escherichia coli* is defined by a wide conformational spectrum. *Appl Environ Microbiol*. 2008;74(23):7431–33.
61. Tsumoto K, Ejima D, Kumagai I, Arakawac T. Practical considerations in refolding proteins from inclusion bodies. *Protein Expr Purif*. 2003;28(1):1–8.
62. Kini R. Molecular moulds with multiple missions: functional sites in three-finger toxins. *Clin Exp Pharmacol Physiol*. 2002;29(9):815–22.
63. Dufton M, Hider R. Conformational properties of the neurotoxins and cytotoxins isolated from Elapid snake venoms. *CRC Crit Rev Biochem*. 1983;14(2):113–71.
64. Kini R, Doley R. Structure, function and evolution of three-finger toxins: mini proteins with multiple targets. *Toxicon*. 2010;56(6):855–67.
65. Ménez A, Bontems F, Roumestand C, Gilquin B, Toma F. Structural basis for functional diversity of animal toxins. *Proceedings of the Royal Society of Edinburgh Section B Biological Sciences*. 1992;99(1-2):83–103.
66. Ménez A. Functional architectures of animal toxins: a clue to drug design? *Toxicon*. 1998 Nov;36(11):1557–72.
67. Khan F, Legler PM, Mease RM, Duncan EH, Bergmann-Leitner ES, Angov E. Histidine affinity tags affect MSP1(42) structural stability and immunodominance in mice. *Biotechnol J*. 2012;7(1):133–47.
68. Drakopoulou E, Zinn-Justin S, Guenneugues M, Gilquin B, Ménez A, Vita C. Changing the Structural Context of a Functional -Hairpin. *J Biol Chem*. 1996;271(20):11979–87.
69. Upadhyay AK, Singh A, Mukherjee KJ, Panda AK. Refolding and purification of recombinant L-asparaginase from inclusion bodies of *E. coli* into active tetrameric protein. *Front Microbiol*. 2014;5:486.
70. Abuhammad A, Lack N, Schweichler J, Staunton D, Sim RB, Sim E. Improvement of the expression and purification of *Mycobacterium tuberculosis* arylamine N-acetyltransferase (TBNAT) a potential target for novel anti-tubercular agents. *Protein Expr Purif*. 2011;80(2):246–52.
71. Girish V, Kumar S, Joseph L, Jobichen C, Kini R, Sivaraman J. Identification and Structural Characterization of a New Three-Finger Toxin Hemachatoxin from *Hemachatus haemachatus* Venom. *PLoS One*. 2012;7(10):e48112.
72. Prieto da Silva A, Yamagushi I, Morais J, Higashi H, Raw I, Ho PL, Oliveira J. Cross reactivity of different specific *Micrurus* antivenom sera with homologous and heterologous snake venoms. *Toxicon*. 2001;39(7):949–53.
73. de Roodt A, Paniagua-Solís J, Dolab J, Estévez-Ramírez J, Ramos-Cerrillo B, Dokmetjian J, Litwin S, Alagón A. Effectiveness of two common antivenoms

- for North, Central and South American *Micrurus* envenomations. J Toxicol Clin Toxicol. 2004;42(2):171–8.
74. Ciscotto PH, Rates B, Silva DAF, Richardson M, Silva LP, Andrade H, Donato MF, Cotta GA, Maria WS, Rodrigues RJ, Sanchez E, De Lima ME, Pimenta AM. Venomic analysis and evaluation of antivenom cross-reactivity of South American *Micrurus* species. J Proteomics. 2011;74(9):1810–25.
75. Fernández J, Alape-Girón A, Angulo Y, Sanz L, Gutiérrez J, Calvete J, Lomonte B. Venomic and antivenomic analyses of the central American coral snake, *Micrurus nigrocinctus* (elapidae). J Proteome Res. 2011;10(4):1816–27.
76. Tanaka G, Sant'Anna O, Marcelino J, Lustoza da Luz A, Teixeira da Rocha M, Tambourgi D. *Micrurus* snake species: venom immunogenicity, antiserum cross reactivity and neutralization potential. Toxicon. 2016;117:59–68.
77. Fry B, Lumsden N, Wüster W, Wickramaratna J, Hodgson W, Kini R. Isolation of a neurotoxin (α -colubritoxin) from a nonvenomous colubrid: evidence for early origin of venom in snakes. J Mol Evol. 2003;57(4):446–52.
78. Lomonte B, Rey-Suárez P, Fernández J, Sasa M, Pla D, Vargas N, Bénard-Valle M, Sanz L, Corrêa-Netto C, Núñez V, Alape-Girón A, Alagón A, Gutiérrez JM, Calvete JJ. Venoms of *Micrurus* coral snakes: Evolutionary trends in compositional patterns emerging from proteomic analyses. Toxicon. 2016;122:7–25.
79. Zaitsev S. Dynamic surface tension measurements as general approach to the analysis of animal blood plasma and serum. Adv Colloid Interface Sci. 2016 Sep;235:201–13.
80. Laustsen AH, Johansen KH, Engmark M, Andersen MR. Recombinant snakebite antivenoms: A cost-competitive solution to a neglected tropical disease? PLoS Negl Trop Dis. 2017;11(2):e0005361.
81. Fernández J, Rey-Suárez P, Pla D, Sanz L, Sasa M, Núñez V, Gutiérrez J, Calvete J, Lomonte B. Proteomic studies on *Micrurus* (coral snakes) venom reveal a dichotomy of phenotypes. Toxicon. 2018;150:319–20.
82. Pruksaphon K, Yuvaniyama J, Ratanabanangkoon K. Immunogenicity of snake α -neurotoxins and the CD4 T cell epitopes. Toxicon. 2022;214:136–44.
83. Mendes TM, Dias F, Horta CCR, Pena IF, Arantes EC, Kalapothakis E. Effective *Tityus serrulatus* anti-venom produced using the Ts1 component. Toxicon. 2008;52(7):787–93.
84. Laustsen AH, Lohse B, Lomonte B, Engmark M, Gutiérrez JM. Selecting key toxins for focused development of elapid snake antivenoms and inhibitors guided by a Toxicity Score. Toxicon. 2015;104:43–5.
85. Borges A, Graham MR, Cândido DM, Pardal PO. Amazonian scorpions and scorpionism: integrating toxinological, clinical, and phylogenetic data to combat a human health crisis in the world's most diverse rainforest. J Venom Anim Toxins incl Trop Dis. 2021;27:e20210028. doi: 10.1590/1678-9199-JVATITD-2021-0028.
86. Arroyo C, Solano S, Segura Á, Herrera M, Estrada R, Villalta M, Vargas M, Gutiérrez JM, León G. Cross-reactivity and cross-immunomodulation between venoms of the snakes *Bothrops asper*, *Crotalus simus* and *Lachesis stenophrys*, and its effect in the production of polyspecific antivenom for Central America. Toxicon. 2017 Nov;138:43–8.
87. de Roodt A, Lanari L, Ramírez J, Gómez C, Barragán J, Litwin S, Henriët van Grootheest J, Desio M, Dokmetjian J, Dolab J, Damin C, Alagón A. Cross-reactivity of some *Micrurus* venoms against experimental and therapeutic anti-*Micrurus* antivenoms. Toxicon. 2021;200:153–64.
88. Ratanabanangkoon K, Tan KY, Eursakun S, Tan CH, Simsirivong P, Pamornsakda T, Wiriyarat W, Klinpayom C, Tan NH. A Simple and Novel Strategy for the Production of a Pan-specific Antiserum against Elapid Snakes of Asia. PLoS Negl Trop Dis. 2016;10(4):e0004565.
89. Chotwivatthanakun C, Pratanaphon R, Akesowan S, Sriprapat S, Ratanabanangkoon K. Production of potent polyvalent antivenom against three elapid venoms using a low dose, low volume, multi-site immunization protocol. Toxicon. 2001;39(10):1487–94.
90. Beghini DG, Damico DC, Da Cruz-Höfling MA, Rodrigues-Simioni L, Delatorre MC, Hyslop S, Marangoni S. Ability of rabbit antiserum against crotapotin to neutralize the neurotoxic, myotoxic and phospholipase A₂ activities of crotoxin from *Crotalus durissus cascavella* snake venom. Toxicol. 2008;22(1):240–8.
91. Fusco LS, Rodríguez JP, Teibler P, Maruñak S, Acosta O, Leiva L. New immunization protocol to produce crotalic antivenom combining *Crotalus durissus terrificus* venom and its PLA2. Biologicals. 2015;43(1):62–70.
92. Laustsen AH, Gutiérrez JM, Knudsen C, Johansen KH, Bermúdez-Méndez E, Cerni FA, Jürgensen JA, Øhlens-chlæger M, Ledsgaard L, Martos-Esteban A, Pus U, Andersen MR, Lomonte B, Engmark M, Pucca MB. Pros and cons of different therapeutic antibody formats for recombinant antivenom development. Toxicon. 2018;146:151–75.